Ultrasonic Levitation Constructing Palladium Doped Near-Infrared Carbon Dots as Nanoprobe for Sensing and Imaging of Carbon Monoxide

Zheng Yang[a,b,c,*] Yaoyao Liu[a], Yuechen Fu[a], Ying Peng[a], Haonan Yang[a], Shaobing Zhang[a], Xiaodan Jia[a,c], Xiangrong Liu[a,c,*] and Jianli Li[b,*]

[a] *College of Chemistry and Chemical Engineering, Xi'an University of Science and Technology, Xi'an 710054, P. R. China.*

[b] *Key Laboratory of Synthetic and Natural Functional Molecule of the Ministry of Education, Xi'an Key Laboratory of Photo-functional Molecular Materials and Theranostic, College of Chemistry & Materials Science, Northwest University, Xi'an, Shaanxi Province 710127, China.*

[c] *Key Laboratory of Coal Resources Exploration and Comprehensive Utilization, Ministry of Land and Resources, Xi'an 710012, P. R. China*

*Corresponding author: yangzheng@xust.edu.cn; liuxiangrongxk@163.com; lijianli@nwu.edu.cn

CONTENTS

1. Experimental section.

General methods

The fluorescent spectra were performed on the Horiba FluoroMax–4 fluorescence spectrophotometer. Absorbance spectra were recorded on the METASH X–8D spectrophotometer. Fluorescent decays were obtained on an Edinburgh FLSP920 steady/transient fluorescence spectrometer. Transmission electron microscope images were performed from a JEM–1400 Flash analyzer. Raman spectra were measured with ThermoFisher DXR 2 spectroscopy. X–ray photoelectron spectroscopy spectra were conducted on a ULVAC–PHI PHI5000VersaProbeIII spectrophotometer with the excitation source of Al Ka. X–Ray powder diffraction spectroscopy analyses were recorded on the Bruker D8 Advance analyzer. IR spectra were performed on a Bruker Tensor 27 spectrometer. Bioimaging of the sensors were conducted on an Olympus FV1000 confocal microscopn. The cell viability was determined using an ELx800 Absorbance Reader (BioTek Instruments, Inc.). Xe lamp irradiation was performed by the CEL–HXF300–T3 Xenon lamp source system.

N-phenyl-o-phenylenediamine, 2,7-dioxynaphthalene, citric acid and CORM-3 were obtained from *Inno– Chem Co., LTD.* (Beijing, China). $PdCl_2$ was obtained from *Kaili Catalyst New Materials CO., LTD*. All other reagents, including various metallic compounds were purchased from *Daosheng Biochemical Science and Trade Co., LTD* (Xi'an, China). Organic reagents and solutions were purchased from *Zhiyuan* and *Tianli Co., LTD* (Tianjin, China). All chemicals are of analytical grade and used without further purification.

Preparation of H_2PdCl_4 Solution

In an analytical balance, 0.8870 g of $PdCl_2$ was accurately weigh and transfer into a 25 mL beaker. Then 3 mL of concentrated hydrochloric acid was added and wait until it is completely dissolved. Then the solution was sonicated for a 5 min to allow the concentrated hydrochloric acid to evaporate. The solution was transferred to in a 5 mL brown volumetric flask and titrated with distilled water until the mark was reached.

Synthesis of the CDs

Ultrasonic levitation: 0.3 g of N-phenyl-o-phenylenediamine, 2,7-dioxynaphthalene and citric acid and 2.00 mL of H_2PdCl_4 solution were added to 30 mL of dimethylformamide (DMF) and stirred until all the solids were dissolved, the solution was treated under ultrasonic levitation conditions with the power of 450 W and resonant frequency of 20 KHz for 5 minutes. After the reaction was completed, the mixture was centrifuged for 10 min (10000 rpm) and the supernatant retained. An equal volume of distilled water was added to the supernatant and dialyzed in a dialysis bag (1000 Da) for 72 h, with water changes every half hour for the first 4 h and every 12 h for the next 68 h, and then the substance in the dialysis bag was frozen under vacuum (~-50 ℃) until it was dried to powder, which is stored in a refrigerator at 0 ℃ for future use.

Solvent heat: 0.3 g of N-phenyl-o-phenylenediamine, 2,7-dioxynaphthalene and citric acid and 2.00 mL of H_2PdCl_4 solution were added to 30 mL of DMF and stirred until all the solids were dissolved, then the solution was transferred to an autoclave lined with polytetrafluoroethylene and heated for 10 h at 200 ℃. After the reaction was completed, the mixture was centrifuged for 10 min (10000 rpm) and the supernatant retained. An equal volume of distilled water was added to the supernatant and dialyzed in a dialysis bag (1000 Da) for 72 h, with water changes every half hour for the first 4 h and every 12 h for the next 68 h, and then the substance in the dialysis bag was frozen under vacuum (~-50 ℃) until it was dried to powder, which is stored in a refrigerator at 0 ℃ for future use.

Microwave: 0.3 g of N-phenyl-o-phenylenediamine, 2,7-dioxynaphthalene and citric acid and 2.00 mL of H_2PdCl_4 solution were added to 30 mL of DMF and stirred until all the solids were dissolved, then the solution was transferred to beaker microwave with the power of 900 W for 60 min. After the reaction was completed, the mixture was centrifuged for 10 min (10000 rpm) and the supernatant retained. An equal volume of distilled water was added to the supernatant and dialyzed in a dialysis bag (1000 Da) for 72 h, with water changes every half hour for the first 4 h and every 12 h for the next 68 h, and then the substance in the dialysis bag was frozen under vacuum

(~-50 ℃) until it was dried to powder, which is stored in a refrigerator at 0 ℃ for future use..

Reflux: 0.3 g of N-phenyl-o-phenylenediamine, 2,7-dioxynaphthalene and citric acid and 2.00 mL of H_2PdCl_4 solution were added to 30 mL of DMF and stirred until all the solids were dissolved, then the solution was transferred to round-bottom flask reflux at 160 ℃ for 12 h. After the reaction was completed, the mixture was centrifuged for 10 min (10000 rpm) and the supernatant retained. An equal volume of distilled water was added to the supernatant and dialyzed in a dialysis bag (1000 Da) for 72 h, with water changes every half hour for the first 4 h and every 12 h for the next 68 h, and then the substance in the dialysis bag was frozen under vacuum (~-50 ℃) until it was dried to powder, which is stored in a refrigerator at 0 ℃ for future use.

Ultrasound: 0.3 g of N-phenyl-o-phenylenediamine, 2,7-dioxynaphthalene and citric acid and 2.00 mL of H_2PdCl_4 solution were added to 30 mL of DMF and stirred until all the solids were dissolved, then the solution was transferred to round-bottom flask ultrasound with the power of for 5 min. After the reaction was completed, the mixture was centrifuged for 10 min (10000 rpm) and the supernatant retained. An equal volume of distilled water was added to the supernatant and dialyzed in a dialysis bag (1000 Da) for 72 h, with water changes every half hour for the first 4 h and every 12 h for the next 68 h, and then the substance in the dialysis bag was frozen under vacuum (~-50 ℃) until it was dried to powder, which is stored in a refrigerator at 0 ℃ for future use.

General procedure

Stock solutions of the CDs (100 mg mL^{-1}) were prepared by dissolving the CDs in 1 mL of dimethyl formamide (DMF) and then diluted to the marked line with distilled water. Stock solutions of the ions were obtained from NaCl, KCl, $AgNO_3$, $BaCl_2$, $CaCl_2$, $MgCl_2$ $6H_2O$, $CdCl_2$ $2.5H_2O$, $MnCl_2$ $5H_2O$, $CoCl_2$ $6H_2O$, $NiCl_2$ $6H_2O$, $ZnCl_2$ $6H_2O$, $PbCl_2$, $HgCl_2$, $CuCl_2$ $2H_2O$, $CrCl_3$ $6H_2O$, anhydrous $FeCl_3$ and $AlC1_3$, $SnCl_4$, Cys (cysteine), Hcy (homocysteine), GSH (glutathione), NaHS, $NaNO_3$, Na_3PO_4, Na_2CO_3, NaOAc, Na_2SO_3, $Na_2C_2O_4$, NaClO, and the ROS and RNS ($O_2^{\cdot-}$, H_2O_2, ·OH, NO, $ONOO^-$) were prepared at 500 μmol·L^{-1} in distilled water. Double distilled water was

used throughout the experiment. All of the detection procedures were performed three times and the reported data were used as the average values.

Sensing of CO.

Fresh stock solutions (1–1000 μmol·L^{-1}) of CORM-3 in deionized water were prepared every time before experiments and kept in a closed vial. For spectroscopic measurements, a required amount of the CORM-3 stock solution was added to the CDs solution (1 mg·mL^{-1}) taken in a cuvette (5 mL) in such a way that the final volume increment remains within less than 1% of the total volume. After the addition of CORM-3, the cap of the cuvette was closed immediately and shook gently to mix thoroughly, and then incubated for the given time prior to spectrometric measurements. The absorptions were recorded at 530 nm and the fluorescence intensities were recorded at 730 nm. The excitation and emission wavelength bandpasses were both set at 5.0 nm and the excitation wavelength was set at 540 nm.

Cytotoxicity testing of the CDs.

MCF-7 cells were cultured in 96-well plates for 24 h at 37 ℃ in 5% CO_2 (the medium was Dulbecco's modified Eagle's medium (DMEM) containing 1% penicillin/ streptomycin and 10% fetal bovine serum). The old DMEM was then removed and fresh DMEM with 100 mL of different concentrations of CDs solution (0–100 mg·mL^{-1}) was added to the cells and incubated for 24 h under the same conditions. Then 10 mL of 3-(4,5)-dimethylthiahiazo(-z-y1)-3,5-di-phenytetrazoliumromide (MTT) solution was added to each well and the incubation was continued for 4 h. Finally, the absorbance of each well was recorded using a microtiter reader to assess the cytotoxicity of the CDs.

Fluorescent imaging of exogenous CO in living cells

Fluorescent imaging was performed in living Mouse fibroblast cells L929. The cells were cultured in Dulbecco's Modified Eagle Medium (DMEM) supplemented with 10% FBS, at 37 ℃ in the humidified atmosphere with 5% CO_2 and 95% air. The cells were then cultured for 4 h until they plated on glass–bottomed dishes. The growth medium was then removed and the cells were washed with DMEM without FBS and imaged. The cells were then incubated with 1 mg·mL^{-1} of the CDs for 30 min at 37 ℃, washed

three times with PBS and imaged. Then the cells were supplemented with 700 μmol·L^{-1} CORM-3 in the growth medium for 30 min at 37 ℃ and imaged.

Fluorescent imaging of endogenous CO in living cells

The living Mouse fibroblast cells L929 were cultured with the same procedure with the imaging experiments of exogenous CO. Then the cells were pretreated with heme for 6 h and then cultured with 1 mg·mL^{-1} of the CDs for 30 min at 37 ℃, washed three times with PBS and imaged.

Fluorescent imaging of drug-induced liver injury in living cells

The living Mouse fibroblast cells L929 were cultured with the same procedure with the imaging experiments of exogenous CO. Then the cells were pretreated with acetaminophen (APAP) 12 h and then cultured with 1 mg·mL^{-1} of the CDs for 30 min at 37 ℃, washed three times with PBS and imaged.

Controlled experiments were performed firstly treated the cells with APAP for 12 h, then pretreated with zinc-protoporphyrin (ZnPP) for 12 h and then cultured with 1 mg·mL^{-1} of the CDs for 30 min at 37 ℃, washed three times with PBS and imaged.

2. Screening of optimum reaction conditions.

Table S1. Screening of various parameters for the optimum reaction conditions

Number	Time (min)	Solvent	Power (kw)	Frequency (KHz)	Emission (nm)
1	1	DMF	450	20	532
2	2	DMF	450	20	597
3	3	DMF	450	20	664
4	4	DMF	450	20	712
5	5	DMF	450	20	730
6	10	DMF	450	20	731
7	15	DMF	450	20	728
8	30	DMF	450	20	728
9	5	H_2O	450	20	553
10	5	Ethanol	450	20	511
11	5	Acetone	450	20	521
12	5	Glycol	450	20	643
13	5	DMSO	450	20	712
14	5	DMF	300	20	723
15	5	DMF	600	20	701
16	5	DMF	750	20	653
17	5	DMF	900	20	642
18	5	DMF	450	5	623
19	5	DMF	450	10	698
20	5	DMF	450	15	710

3. Optical properties of the CDs.

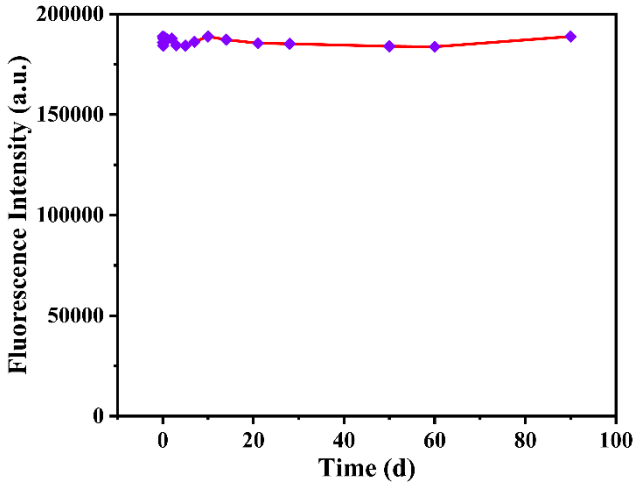

Figure S1. Time–stability for the fluorescence intensity of CDs solution, λ_{ex} = 530 nm.

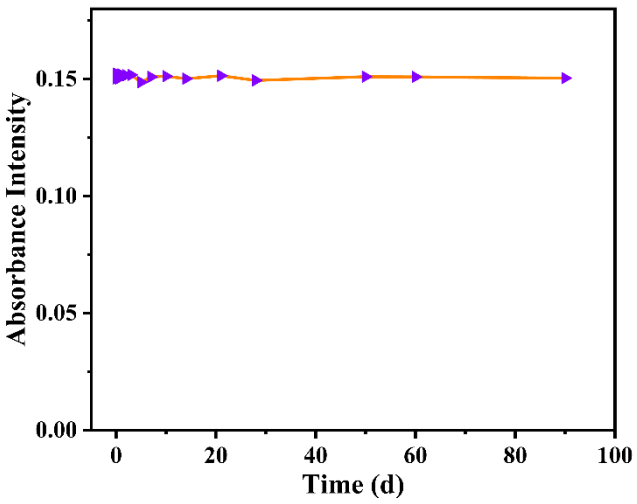

Figure S2. Time–stability for the absorption intensity of the CDs solution.

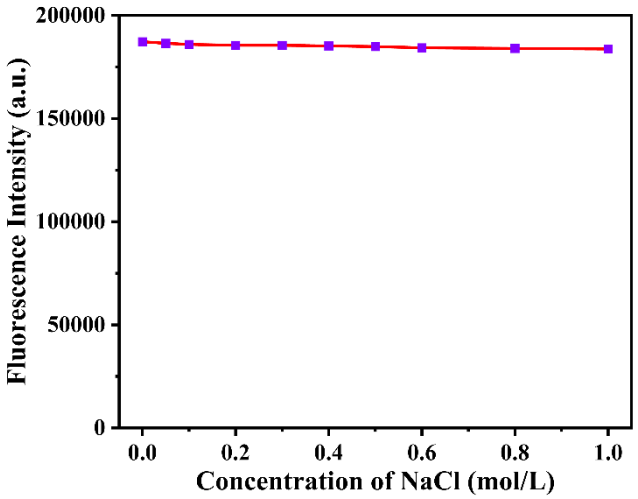

Figure S3. Effect of ionic strength of NaCl on fluorescent intensity of the CDs, λ_{ex} = 530 nm.

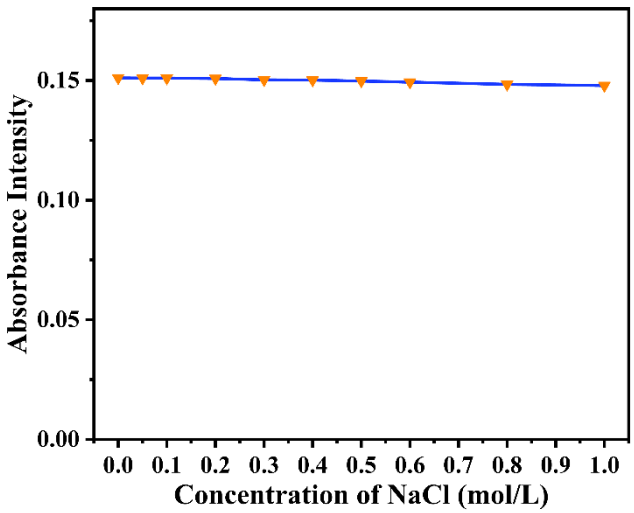

Figure S4. Effect of ionic strength of NaCl on absorption intensity of the CDs.

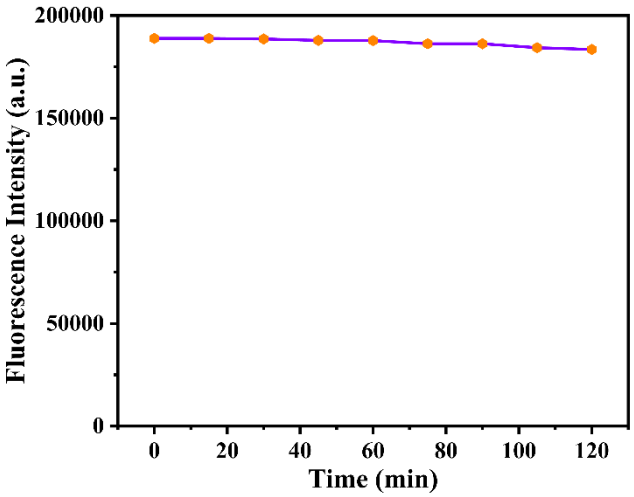

Figure S5. Effect of time intervals with UV irradiation at 365 nm on fluorescent intensity of the CDs, λ_{ex} = 530 nm.

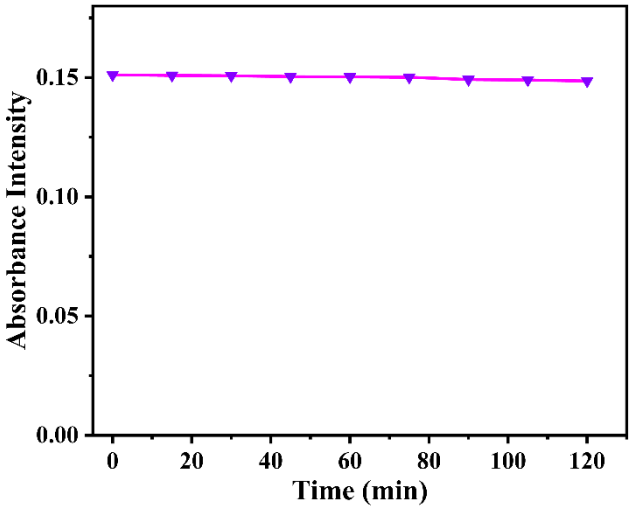

Figure S6. Effect of time intervals with UV irradiation at 365 nm on absorption intensity of the CDs.

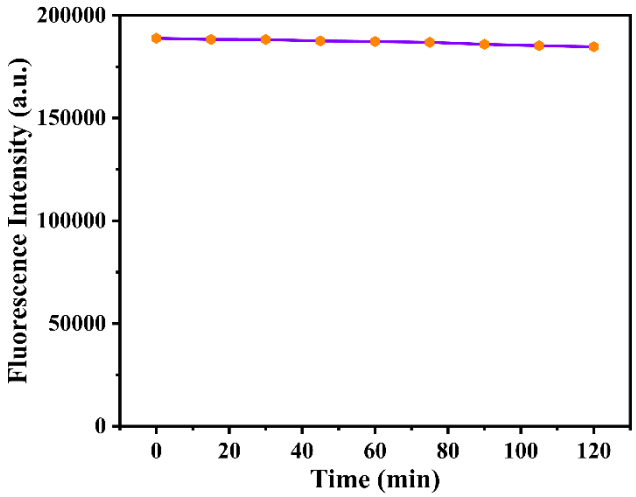

Figure S7. Effect of time intervals with Xe irradiation with the light intensity of 1500 mW/cm^2 on fluorescent intensity of the CDs, λ_{ex} = 530 nm.

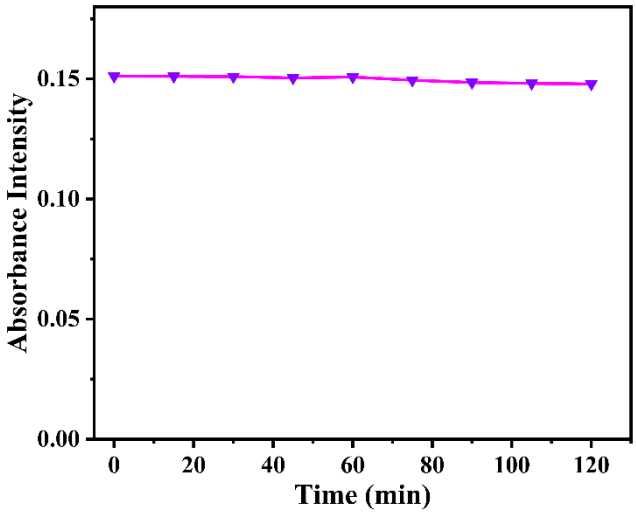

Figure S8. Effect of time intervals with Xe irradiation with the light intensity of 1500 mW/cm^2 on absorption intensity of the CDs.

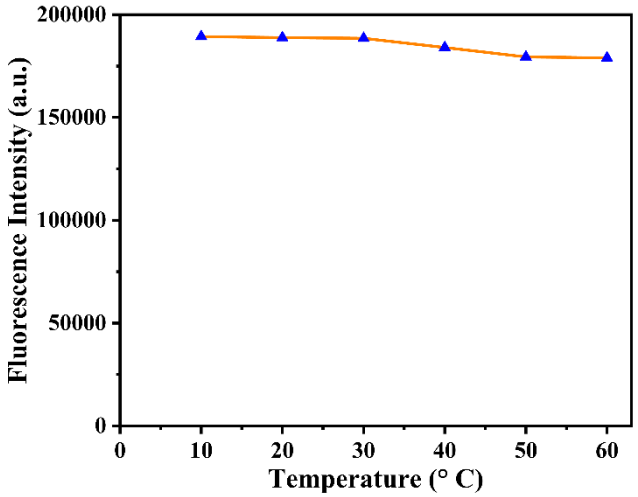

Figure S9. The fluorescence stability of the CDs in high temperature, λ_{ex} = 530 nm.

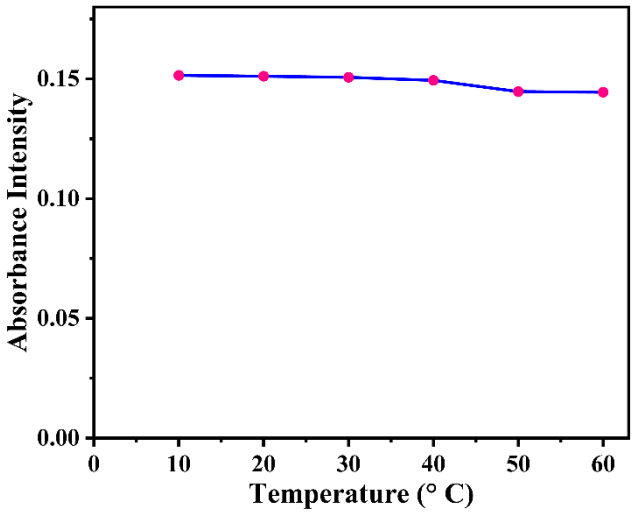

Figure S10. The absorption stability of the CDs in high temperature.

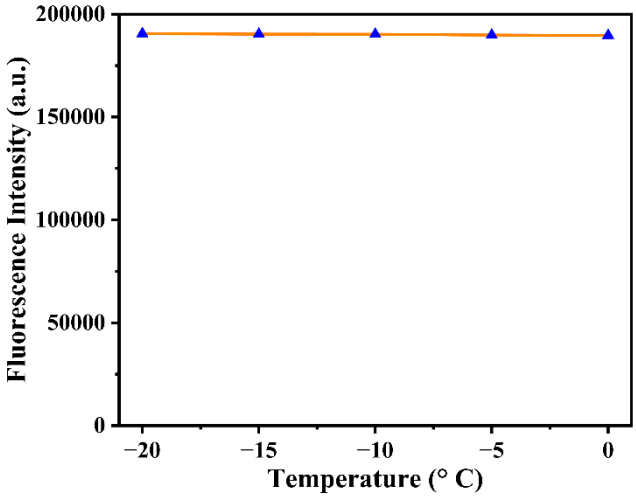

Figure S11. The fluorescence stability of the CDs in low temperature, λ_{ex} = 530 nm.

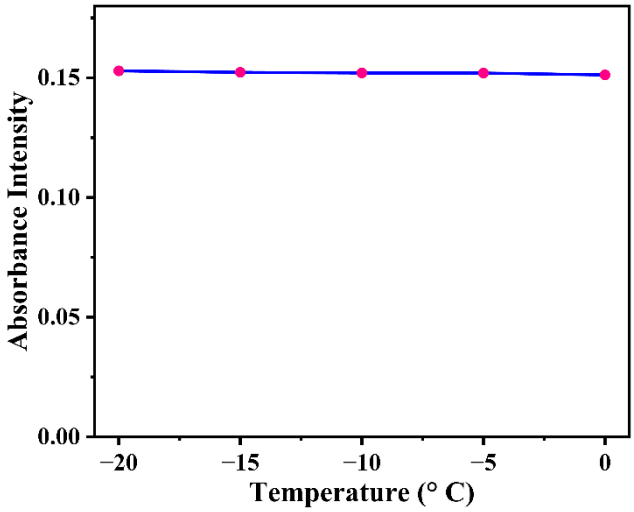

Figure S12. The absorption stability of the CDs in low temperature.

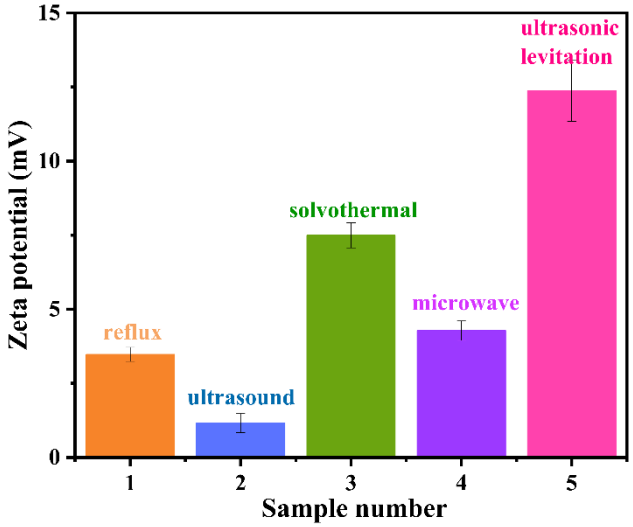

Figure S13. Zeta potential of Pd-CDs from each synthetic method.

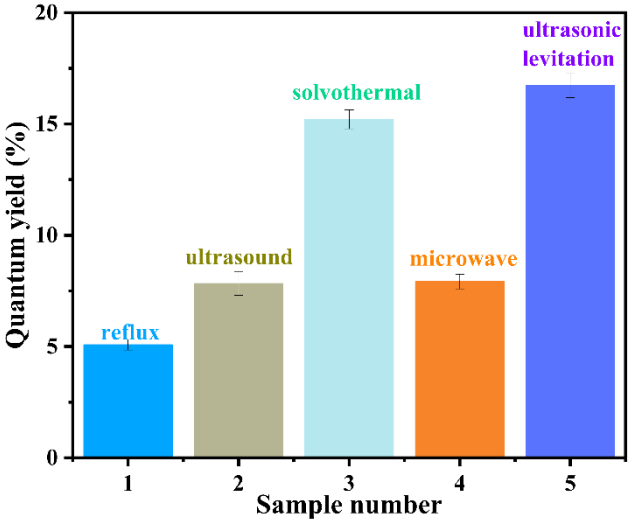

Figure S14. Fluorescence quantum yields of Pd-CDs from each synthetic method.

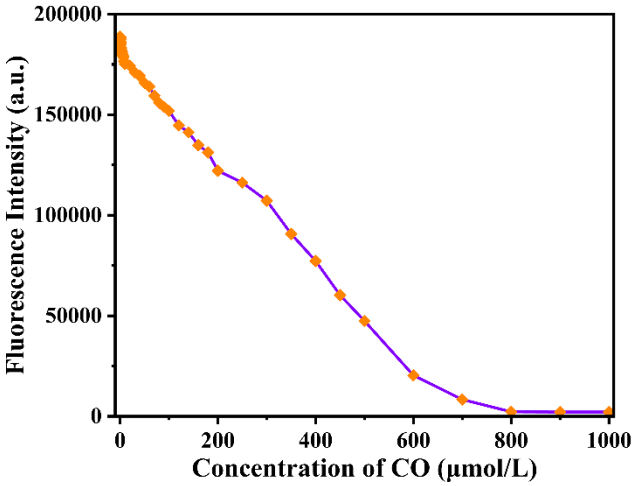

Figure S15. Fluorescence intensity of Pd-CDs (1 mg·mL^{-1}) upon addition of CO, λ_{ex} = 530 nm.

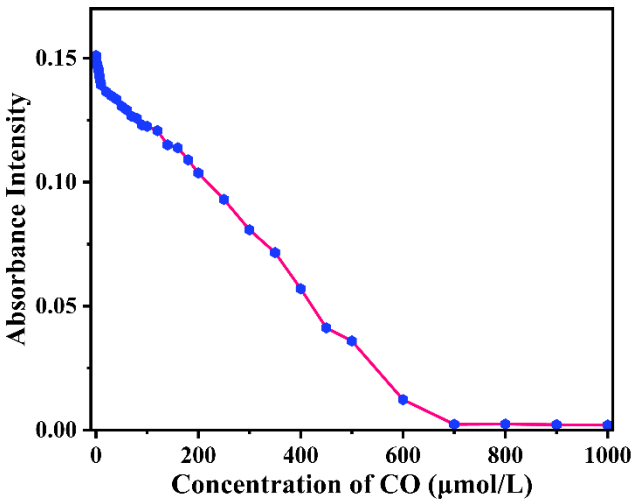

Figure S16. Fluorescence intensity of Pd-CDs (1 mg·mL^{-1}) upon addition of CO, λ_{ex} = 530 nm.

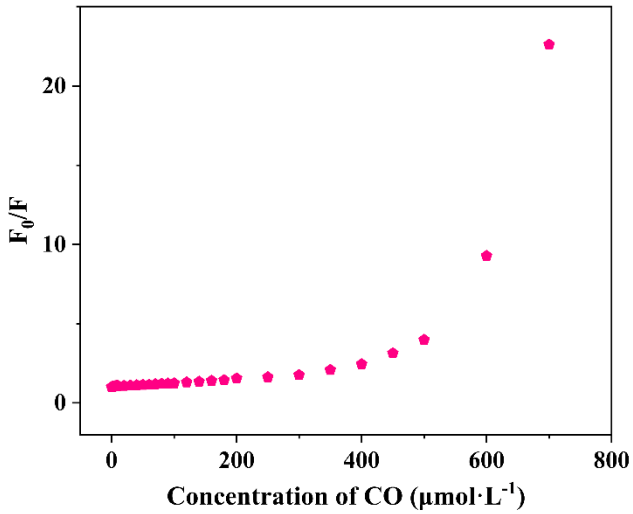

Figure S17. Stern-Volmer plot of the Pd-CDs (1 mg·mL^{-1}) in the presence of CO (0-700 μmol·mL^{-1}).

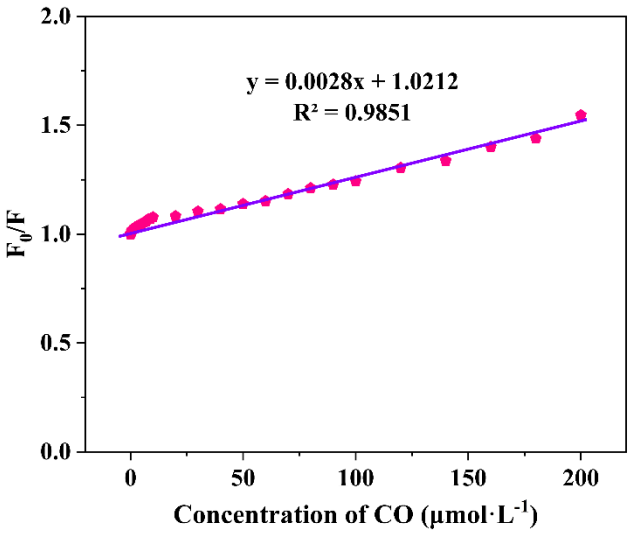

Figure S18. Stern-Volmer plot of the Pd-CDs (1 mg·mL^{-1}) in the presence of CO (0-200 μmol·mL^{-1}).

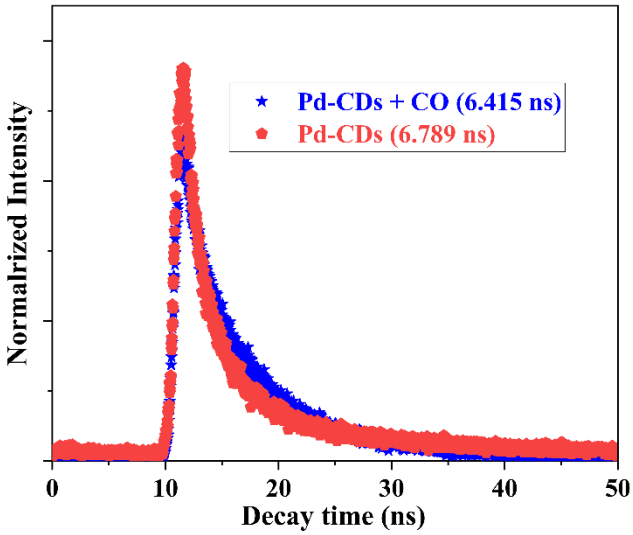

Figure S19. Fluorescence decay time of Pd-CDs in the presence of CO.

4. Equations

4.1 Equations for calculation of fluorescence lifetime

$$\tau=\tau_1 B_1 + \tau_2 B_2$$

B_1, B_2 stand for fractional intensities; τ_1, τ_2 are decay times.

4.2 Equations for calculation of quantum yield

$$\varphi_S = \varphi_R \frac{F_S A_R}{F_R A_S} \frac{\eta_S^2}{\eta_R^2}$$

ϕ stands for the fluorescence quantum yield, *F* refers to the integrated fluorescence intensity, and *A* is the absorption values. The subscript "*R*" and "*S*" correspond to the reference and the sample.

4.3 Equations for calculation of LOD

The detection limits were estimated based on the Kaiser's definition:

$$y_d = y_b - KS_b \text{ (on-off)}$$

y_d is the detection limit of the sample. y_b present the mean value fluorescence intensity of the blank samples. S_b is the population standard deviation of the blank. The K value is 3 (M. Belter, A. Sajnog, D. Baralkiewicz, *Tlanta*, 2014, **129**, 606.).

Table S2. Fluorescence intensity and Standard deviation of blank samples

Probe	Fl. Intensity	Mean value	Standard deviation	$y_d = y_b - KS_b$
Blank #1	188870	188860.3	95.70214	188587
Blank #2	188892			
Blank #3	188782			
Blank #4	188883			
Blank #5	188923			
Blank #6	188998			
Blank #7	188639			
Blank #8	188842			
Blank #9	188910			
Blank #10	188864			

[a] y_d is the detection limit of the sample. y_b present the mean value fluorescence intensity of the blank samples. S_b is the population standard deviation of the blank. The K value is 3.

Table S3. Fluorescent intensity and corresponding concentration of HClO.

[CORM-3] ($\mu mol \cdot L^{-1}$)	Fl. Intensity
0.1	188870
0.2	188553
0.3	188216
0.4	187885
0.5	187527
0.6	186451
0.7	185913
0.8	185632
0.9	185321
1	185012
2	183241
3	182124
4	181263
5	180274
6	179284
7	178432
8	176583
9	176352
10	175241

5. MTT assay results of the probe.

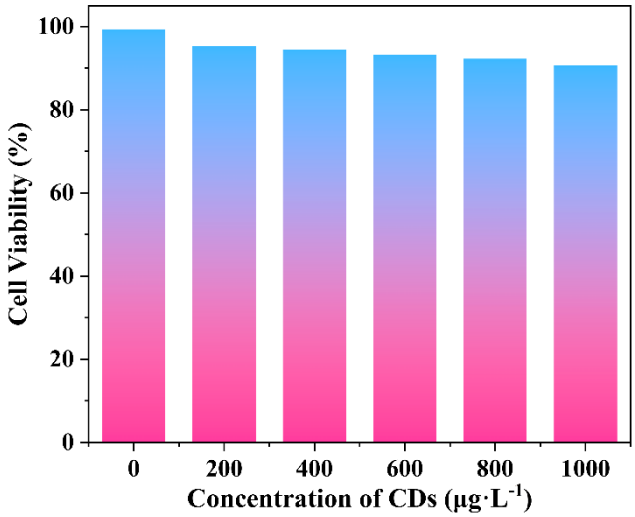

Figure S20. Cells viability value on the concentration of the CDs for MCF-7 cell.

Table S4. MTT assay results, calculated inhibition ratio and cells viability value of the CDs for MCF-7 cell.

[CDs]/mg·mL^{-1}	1	2	3	Average	Inhibition ratio	Cells viability
0	0.473	0.456	0.457	0.4620	0.0063	99.37%
200	0.445	0.451	0.434	0.4433	0.0464	95.36%
400	0.456	0.427	0.435	0.4393	0.0550	94.50%
600	0.438	0.442	0.421	0.4337	0.0672	93.28%
800	0.425	0.435	0.427	0.4290	0.0773	92.27%
1000	0.428	0.419	0.417	0.4213	0.0937	90.63%

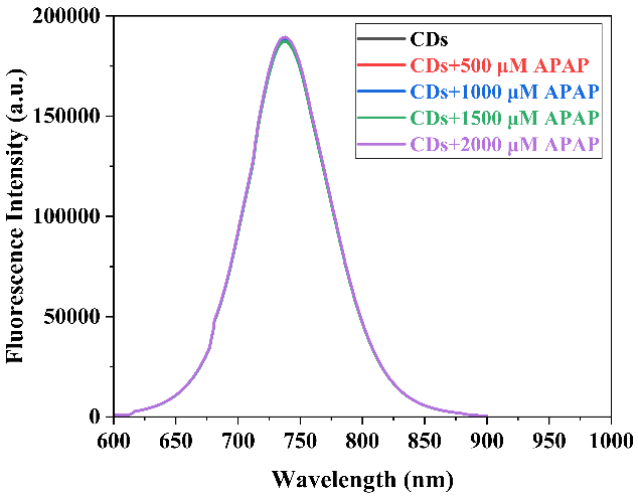

Figure S21. Fluorescence detection of Pd-CDs (1 mg mL^{-1}) upon addition of different concentration of APAP. λ_{ex} = 530 nm.

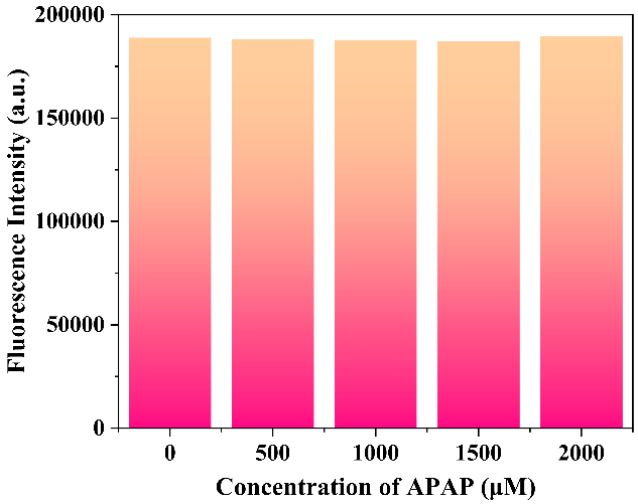

Figure S22. Fluorescence intensity of Pd-CDs (1 mg mL^{-1}) upon addition of different concentration of APAP. λ_{ex} = 530 nm.

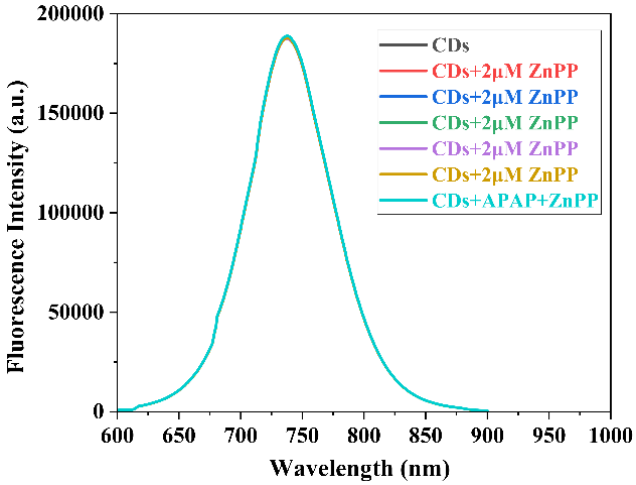

Figure S23. Fluorescence detection of Pd-CDs (1 mg·mL^{-1}) upon addition of different concentration of ZnPP and the APAP (2000 μmol·L^{-1})-ZnPP (10 μmol·L^{-1}) mixture. λ_{ex} = 530 nm.

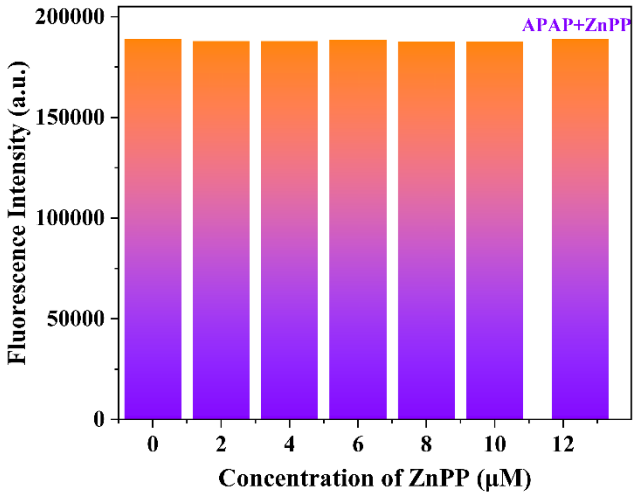

Figure S24. Fluorescence intensity of Pd-CDs (1 mg·mL^{-1}) upon addition of different concentration of ZnPP and the APAP (2000 μmol·L^{-1})-ZnPP (10 μmol·L^{-1}) mixture. λ_{ex} = 530 nm.

6. Comparison of fluorescent probes for detecting CO.

Table. S5 Comparison of fluorescent probes for detecting CO

Probe	LOD	Linear range	Response time	Application	Reference
HBT - CORM3	0.11 μM	0-175 μM	15 min	Rapid detection of CORM-3; imaging in living cells and zebrafish	[1]
HPQ-BI-CO	0.03 μM	0.1-100.0 μM	120 s	Detection of exogenous/endogenous carbon monoxide in living 4T1 cells; in vivo visualization of CO in zebrafish	[2]
NAP-CO	19.8 nM	1-30 μM	30 min	Detection of CO in living cells, tissues, zebrafish and mice	[3]
Z1CO	0.84 μM	0-10 μM	60 min	Detection and imaging of endogenous/exogenous CO; monitoring of Cd^{2+} in plants	[4]
ABT-Ally-CO	12.5 nmol/L	0-40 μmol/L	30 min	Detection and imaging of endogenous/exogenous CO	[5]
Probe 1	58 nM	0-35 μM	20 min	Detection of CO in air, aqueous solutions, and living cells	[6]
NIR-RB-CO	0.135 μM	0-8 μM	15 s	Noninvasive imaging of endogenous and exogenous CO both in vitro and in vivo	[7]
TPANN-Pd	160 nM (CORM-3); 1.7 ppb (CO vapor)	0~150 μM 0~4.5%	1 min	Sensing CO at room temperature; imaging CO in living cells	[8]
CORM3-NIR	70 nM	0-12 μM	20 min	Detection of CORM-3 in the life system	[9]
COP-3E-Py	-	0-50 μM	60 min	Imaging of endogenous CO release in live cell and brain settings	[10]
BTHC-CO	25 nM	0-15 μM	15 min	In vitro detection and intracellular imaging of CO	[11]
HFCO-1	0.06 μM	0−8 μM	20 min	cell imaging of CO in living cells	[12]

1-Ac	50 nM	0~200 μM	30 min	Tracking endogenous CO in zebrafish embryos and mouse tissues	[13]
MPVC-I MPVC-II	100 ppm	-	10 min	Sensing gaseous CO; detection of blood HbCO levels	[14]
Hcy-Rh	0.36 μM	0~200 μM	-	Detection of CO alongside small viscosity changes in organelles of live cells	[15]
NFCOP	0.32 μmol/L	-	10 s	Imaging of CO both in vitro and in vivo	[16]
N-CQDs	0.07μM	4.77-41.23μM	30 s	The real-time detection of atmospheric CO	[17]
N-CQDs	0.102 μM	2.43–47.51 μM	-	Detection of trace amounts of CO in plant cells	[18]
Pd-CDs	**0.19 nM**	**0~800 μM**	**10 s**	**Endogenous and exogenous CO sensing and imaging**	**This paper**

References

1. L. Q. Yan, C. P. Zhou and H. Yang, *Sens. Actuators B Chem.*, 2023, **382**, 133492.
2. Y. S. Xia, L. Yan, G.J. Mao, W. L. Jiang, W. X. Wang, Y. F. Li, Y. Q. Jiang and C. Y. Li, *Sens. Actuators B Chem.*, 2021, **340**, 129920.
3. L. Z. Yue, Y. H. Tang, H. W. Huang, W. H. Song and W. Y. Li, *Sens. Actuators B Chem.*, 2021, **344**, 130245.
4. H. S. Zhai, Y. Y. Zhang, D. H. Tian, Z. Y. Shang, M. M. Wu, Z. Q. Zhang, Q. T. Meng and R. Zhang, *J. Hazard. Mater.*, 2025, **495**, 139135.
5. M. Liu, B. Feng, F. Y. Chu, D. Y. Fan, F. Zheng, F. Chen and W. B. Zeng, *Chin. Chem. Lett.*, 2025, **36**, 110043.
6. W. Y. Feng, J. X. Hong and G. Q. Feng, *Sens. Actuators B Chem.*, 2017, **251**, 389-395.
7. Y. Liu, P. P. Wang, X. L. Shi, K. Yang, M. Deng, H. L. Zhang, Z. B. Zhai, D. Cheng, L. W. He and S. J. Li, *Sens. Actuators B Chem.*, 2026, **449**, 139127.
8. X. K. Fang, Z. H. Zhang, Y. Y. Qi, B. B. Yue, J. H. Yu, H. Yang and Haitao Yu, *Anal. Chem.*, 2023, **95**, 11518-11525.
9. E. B. Zhou, S. Y. Gong, Q. F. Xia and G. Q. Feng, *ACS Sens.*, 2021, **6**, 1312-1320.

10. J. Morstein, D. Hofler, K. Ueno, J. W. Jurss, R. R. Walvoord, K. J. Bruemmer, S. P. Rezgui, T. F. Brewer, M. Saitoe, B. W. Michel, C. J. Chang, *J. Am. Chem. Soc.*, 2020, **142**, 15917-15930.
11. W. Feng, D. Liu, Q. Zhai, G. Feng, *Sens. Actuators B Chem.*, 2017, **240**, 625-630.
12. M. Sun, H. Yu, K. Zhang, S. Wang, T. Hayat, A. Alsaedi, D. Huang, *ACS Sens.*, 2018, **3**, 285-289.
13. K. Liu, X. Kong, Y. Ma, W. Lin, *Angew. Chem. Int. Ed.*, 2017, **56**, 13489-13492.
14. G. Shi, T. Yoon, S. Cha, S. Kim, M. Yousuf, N. Ahmed, D. Kim, H. W. Kang, K. S. Kim, *ACS Sens.*, 2018, **3**, 1102-1108.
15. J. A. Robson, M. Kubánková, T. Bond, R. A. Hendley, A. J. P. White, M. K. Kuimova, J. D. E. T. Wilton-Ely, *Angew. Chem. Int. Ed.*, 2020, **59**, 21431-21435.
16. G. Ma, Q. Ding, Y. Zhang, Y. Wang, J. Xiang, M. Li, Q. Zhao, S. Huang, P. Gong, J. S. Kim, *Chin. Chem. Lett.*, 2024, **35**, 109293.
17. S. Mondal, P. Sahoo, *J. Mater. Chem. C*, 2025, **13**, 19842-19847.
18. S. Mondal, O. Sarkar, S. M. Mandal, A. Chattopadhyay, P. Sahoo, *Dalton Trans.*, 2025, **54**, 8214-8223.